J. Fluid Mech. (1999), *vol.* 382, *pp.* 137–154. Printed in the United Kingdom

© 1999 Cambridge University Press

Kinematic dynamo action in a network of screw motions; application to the core of a fast breeder reactor

By F. PLUNIAN, P. MARTY AND A. ALEMANY

Laboratoire des Ecoulements Géophysiques et Industriels, P.B. 53, 38041 Grenoble, France

(Received 8 October 1997 and in revised form 15 September 1998)

Most of the studies concerning the dynamo effect are motivated by astrophysical and geophysical applications. The dynamo effect is also the subject of some experimental studies in fast breeder reactors (FBR) for they contain liquid sodium in motion with magnetic Reynolds numbers larger than unity. In this paper, we are concerned with the flow of sodium inside the core of an FBR, characterized by a strong helicity. The sodium in the core flows through a network of vertical cylinders. In each cylinder assembly, the flow can be approximated by a smooth upwards helical motion with no-slip conditions at the boundary. As the core contains a large number of assemblies, the global flow is considered to be two-dimensionally periodic. We investigate the self-excitation of a two-dimensionally periodic magnetic field using an instability analysis of the induction equation which leads to an eigenvalue problem. Advantage is taken of the flow symmetries to reduce the size of the problem. The growth rate of the magnetic field is found as a function of the flow pitch, the magnetic Reynolds number (Rm) and the vertical magnetic wavenumber (k). An α-effect is shown to operate for moderate values of Rm, supporting a mean magnetic field. The large-Rm limit is investigated numerically. It is found that $\alpha = O(Rm^{-2/3})$, which can be explained through appropriate dynamo mechanisms. Either a smooth Ponomarenko or a Roberts type of dynamo is operating in each periodic cell, depending on k. The standard power regime of an industrial FBR is found to be subcritical.

1. Introduction

1.1. *MHD studies in the FBR*

The fast breeder reactors (FBR) are cooled with liquid sodium which has a high electrical conductivity ($4 \times 10^6\ \Omega^{-1}\ \mathrm{m}^{-1}$ at 500 °C). Owing to the large size and velocity of an FBR, the magnetic Reynolds numbers (Rm) calculated for different parts of the reactor are found to be much larger than unity. For instance, the typical dimensions of length and velocity relevant to the sodium flow in the core, are 1 m and 5 m s^{-1} leading to $Rm = 25$ at 500 °C. Then, at first sight, some MHD phenomena of dynamo type could take place in an FBR, with a transfer of mechanical energy (from the pumps) into magnetic energy. This effect has been pointed out by Bevir (1973) and was also the subject of a note by M. Steenbeck (1973) to the Soviet Academy of Sciences (private communication from K.-H. Rädler). This effect might be undesirable for the smooth running of the reactors (e.g. increased charge losses and disturbances of the sodium motion resulting from the

back reaction of the magnetic field through the Lorentz forces, and electromagnetic strains on the structures). Experimental measurements have been done in the FBR BN600 (Kirko *et al.* 1982), in the FBR Phenix (Werkoff & Garnier 1988) and more recently in the FBR Superphenix (Alemany *et al.* 1998). Until now, no dynamo effect has been experimentally observed. Nevertheless, the core of an FBR has never been the subject of electromagnetic measurements, essentially because the high temperatures (500 °C) and the neutronic flux make it hostile to the usual electromagnetic probes. The motivation of this paper is to evaluate theoretically the possibility of dynamo action in the core of an FBR for the ideal case of a homogeneous electromagnetic medium. The data used in this paper correspond to the FBR Phenix.

1.2. *Dynamo effect*

In a homogeneous medium, the Maxwell equations in the MHD approximation yield the induction equation

$$\partial_t \boldsymbol{B} = \nabla \times (\boldsymbol{u} \times \boldsymbol{B}) + Rm^{-1}\nabla^2 \boldsymbol{B}, \quad \text{with } \nabla \cdot \boldsymbol{B} = 0, \tag{1.1a,b}$$

written in its dimensionless form, where $\boldsymbol{B}$ and $\boldsymbol{u}$ are the magnetic and velocity fields. The dimensionless parameter Rm is the magnetic Reynolds number, defined by

$$Rm = \sigma \mu U L, \tag{1.2}$$

where σ denotes the electrical conductivity, μ the magnetic permeability, U and L characteristic scales of speed and length relevant respectively to the flow and the magnetic field. We speak of a kinematic dynamo provided that the $\boldsymbol{B}$-field solution of (1.1) is growing exponentially in time. For a given geometry of the velocity field, the growth of the magnetic field is generally obtained above a threshold of Rm called the critical magnetic Reynolds number. Therefore, to know whether a dynamo effect is possible inside the core of an FBR, knowledge of the geometry, electromagnetic properties and intensity of the sodium flow is of primary interest. (For reviews on dynamo theory, see e.g. Moffatt 1978; Krause & Rädler 1980; Childress & Gilbert 1995.)

1.3. *Description of the core flow*

The core of an FBR (figure 1*a*) is composed of more than one hundred vertical cylinders of hexagonal cross-section. In each cylinder assembly (figure 1*b*), the liquid sodium flows between vertical rods (figure 1*c*) which contain the nuclear fuel. On its way up, the sodium flow receives the heat resulting from the nuclear reactions, and this energy is released after the sodium has left the core through specific heat exchangers. Each assembly contains more than two hundred rods. In order to ensure sufficient space between the rods and enable the sodium to flow between them and be heated, a helical space wire is wound around each rod.

A study of the flow pattern has been done by Lafay, Meunant & Barroil (1975) in the simple case of one 19-rod assembly. They obtained numerical and experimental results summarized in figure 2. A map of the ratio of the horizontal to the vertical velocity field components (U_H/U_Z) is given in a horizontal cross-section, for a given flow rate. The maximum horizontal velocity (63% of U_Z) is significantly larger than the value predicted assuming that the flow follows the wire wrap angle (16% of U_Z).

In the case of a 217-rod assembly, it would be a hard task to determine the motion in detail, either experimentally or numerically. This is why we shall consider, in this paper, an idealized velocity field, keeping the main geometrical features of the core

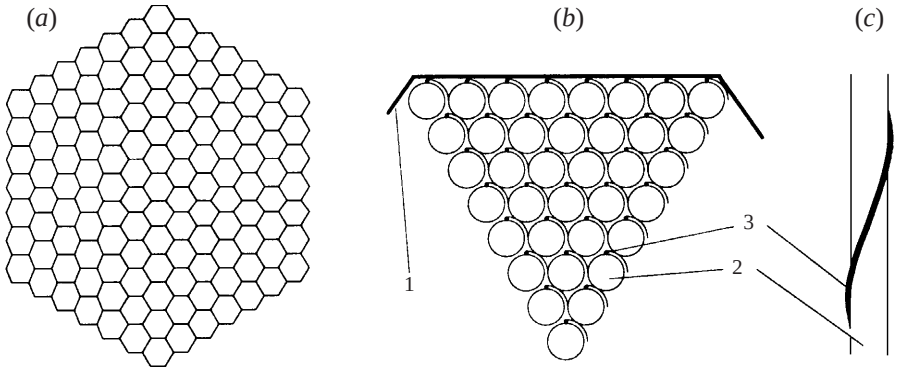

FIGURE 1. (*a*) The core containing 121 assemblies arranged in a honeycomb structure (horizontal section). (*b*) One assembly (only one sixth of) containing 217 rods (horizontal section). (*c*) One rod (vertical section). A helical space wire (3) is wrapped around each rod (2). The sodium is constrained to flow within the boundaries (1) of each assembly.

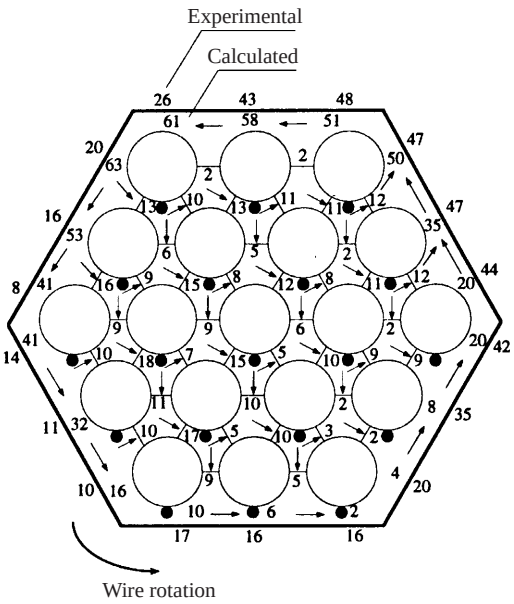

FIGURE 2. One assembly containing only 19 rods for the experimental investigation of Lafay *et al.* (1975). The numbers represent the ratios of the horizontal to the vertical velocity field components U_H/U_Z, in %.

flow which are known to play an important role in dynamo action. The first feature is a non-zero mean helicity which is known to enhance dynamo action. It exists at the length scale of one assembly and also at the smaller length scale of one rod, due to the helical space wire. The second feature is the two-dimensionally periodic arrangement of the assemblies and rods.

1.4. *Outline*

The analytical expression for an ideal incompressible flow satisfying the two previous features (helicity and two-dimensionally periodicity) is introduced in §2.1. It is made

up from a two-dimensionally periodic network of smooth helical motions. Two related types of dynamo mechanisms are investigated in the light of classic results of dynamo theory (§2.2). The mathematical model leading to an eigenvalue problem is developed (§3.1), and advantage is taken of the symmetries of the flow to reduce the size of the problem (§3.2). In the case where a mean magnetic field exists, an α-effect is derived (§3.3). On the basis of asymptotic analysis results, it is shown that in the limit of large Rm, $\alpha = O(Rm^{-2/3})$. Some numerical results are presented (§4) for a wide range of Rm up to 2^{12}, enforcing the theoretical predictions of §2.2 and §3.3.

The numerical results concerning the parameters of an FBR core flow are finally presented (§5). In that case, the ideal flow of §2.1 represents the mean flow in the core, at the length scale of either one assembly or one rod.

2. The velocity field

2.1. *Analytical expression*

We consider a solenoidal velocity field of the form

$$\boldsymbol{u} = \nabla\psi(x, y) \times \hat{\boldsymbol{z}} + w(\psi)\hat{\boldsymbol{z}}, \tag{2.1}$$

where x and y (and, below, z) are the dimensionless Cartesian coordinates, $\hat{\boldsymbol{z}}$ the unit vector in the z-direction and ψ the stream function of the flow. This class of steady flows, two-dimensionally periodic and with the vertical z-velocity being constant on stream surfaces, has been the subject of intensive study, starting with the pioneering work of Roberts (1970, 1972). He found that, for $w = \psi = \cos x - \cos y$ (referred to as the Roberts flow), dynamo action occurs. A corresponding α-effect has also been derived. Childress (1979) generalized this result to any non-negative function ψ vanishing on the boundary, with natural periodic boundary conditions for the magnetic field, and $Rm \gg 1$. With an appropriate boundary layer analysis, he found that $\alpha = O(Rm^{-1/2})$ in the limit of large Rm, provided that $\nabla^2\psi(x, y) < 0$. The possibility of fast dynamo action has been investigated by Soward (1987), modifying the Roberts flow by adding vorticity field singularities placed at the X-type stagnation points of the flow (see also Soward 1989). The α-effect for a family of cat's-eye flows defined by $\psi = \sin x \sin y + \delta \cos x \cos y$ has been investigated by Childress & Soward (1989). Recently, Tilgner & Busse (1995) studied the dynamo action of the Roberts flow at moderate Rm (up to 40) for some specific subharmonic magnetic modes. Their work was motivated by a laboratory dynamo experiment (Busse *et al.* 1996; Rädler, Apstein & Schüler 1997).

For our purpose, we consider a family of spiralling vortices with a non-negative velocity in the z-direction, defined by (2.1) and

$$w(x, y) = K\psi, \quad \psi(x, y) = a(1 + \cos x)(1 + \cos y), \tag{2.2}$$

where K and a are positive coefficients. This field differs from the Roberts flow for which the screw-sense of each cell is identical but the direction of flow alternates between one cell and its immediate neighbour.

2.2. *Dynamo mechanisms*

2.2.1. *Dynamo of Roberts type*

The flow (2.2) is equal to zero at the cell boundaries. This defines a set of stagnation points corresponding to $\psi = 0$, located at $x = (2n + 1)\pi$ and $y = (2m + 1)\pi$, with n and m integers. The cell corners are high-order stagnation points, the character of

which is quantified as follows. The Lagrangian variables $x(x_0, y_0, t), y(x_0, y_0, t)$ of the flow (2.2) satisfy

$$\partial_t(x, y) = 4ac\left(-\sin\frac{y}{2}\cos\frac{x}{2}, \sin\frac{x}{2}\cos\frac{y}{2}\right), \tag{2.3}$$

where c is a coefficient defined by the initial condition at time $t = t_0$

$$\cos\frac{x(t)}{2}\cos\frac{y(t)}{2} = \cos\frac{x(t_0)}{2}\cos\frac{y(t_0)}{2} = c. \tag{2.4}$$

For symmetry reasons, it is sufficient to consider one quarter of the primary cell, e.g. $(x, y) \in [0, \pi]^2$. Then, (2.3) and (2.4) imply that

$$\partial_t x = -4ac\left(\cos^2\frac{x}{2} - c^2\right)^{1/2}, \quad \partial_t y = 4ac\left(\cos^2\frac{y}{2} - c^2\right)^{1/2}. \tag{2.5a,b}$$

Now, provided that $2|c| \leqslant |x - \pi| \ll 1$, and for $(x, y) = (\pi - 2c, 0)$ at $t = t_0$, we have

$$x = \pi - 2c\,\cosh[2ac(t - t_0)]. \tag{2.6}$$

The x-component of a particle frozen in the fluid at the vicinity of the corner (π, π) is then stretched exponentially as $t \to \infty$, while the y-component is contracted. Therefore, we would expect generation of magnetic field in sheets connecting the corners and aligned with the cell boundaries. Let δ be the flux sheet width and assume $\delta \ll 1$. Then the horizontal velocity in the sheet is $O(\delta)$, yielding an effective magnetic Reynolds number δRm. The sheet width is then $\delta = O(\delta Rm)^{-1/2}$, which implies

$$\delta = O(Rm^{-1/3}). \tag{2.7}$$

From (2.2), we have also

$$\psi \sim \delta^2 = O(Rm^{-2/3}). \tag{2.8}$$

Now we can estimate the time a particle takes to turn through $\pi/4$ rad. This corresponds to $x = y$ implying from (2.4) that $x = \pi - 2c^{1/2}$. When replaced in (2.6) this gives the time τ_C for a fluid particle to complete a circuit of the cell:

$$\tau_C \sim \frac{2}{ac}\ln(1/c), \tag{2.9}$$

which, when applying the relation $\psi = 4ac^2$ and (2.8), leads to

$$\tau_C \sim \frac{2}{(a\psi)^{1/2}}\ln\frac{4a}{\psi} = O(Rm^{1/3}\ln Rm). \tag{2.10}$$

This convection time scale may be compared to the diffusion time scale $\tau_D \sim \delta^2 Rm = O(Rm^{1/3})$, which stresses the slow dynamo tendency. This is in agreement with Theorem 6.1 in Childress & Gilbert (1995) which excludes from the class of fast dynamos any steady smooth two-dimensional flow.

2.2.2. *Dynamo of Ponomarenko type*

The straight lines $(x, y) = (2n\pi, 2m\pi)$ determine the axes around which the spiralling motions are developed. In the vicinity of such an axis, the flow consists of solid-body helical motion. This can be seen e.g. in the vicinity of the axis $x = y = 0$, considering the expression for the velocity field (2.2) with respect to dimensionless cylindrical coordinates (r, θ, z). At first order in r, we have $(u_r, u_\theta, u_z) = (0, 2ar, 4Ka)$. It is a solid-body helical motion with pitch $\chi = u_z/(u_\theta)_{r=1} = 2K$.

The single screw motion $\boldsymbol{u} = (0, r\omega(r), W(r))$ has been the object of much investigation in dynamo theory, starting with Ponomarenko (1973). The solid-body motion has been shown to be a fast dynamo (Gilbert 1988) whereas the smooth motion belongs to a wide class of slow dynamos (Soward 1990). Both have been investigated as the basis of the realization of an experimental dynamo (Gailitis *et al.* 1987; Gailitis 1993). In the limit of large Rm, the behaviour of the magnetic field has been analysed asymptotically both in the kinematic frame (Gilbert 1988; Ruzmaikin, Sokoloff & Shukurov 1988) and in the dynamical frame (Bassom & Gilbert 1997). We now summarize a few of the results, obtained with the kinematic asymptotic approach for the smooth Ponomarenko flow, that will be useful in this paper. In the limit of large Rm, the maximum growth rate of the magnetic field and the corresponding azimuthal and vertical modes satisfy

$$p_{max} = O(Rm^{-1/3}), \quad m_{max}, k_{max} = O(Rm^{1/3}). \tag{2.11}$$

The magnetic field is localized in a layer of thickness $\delta = O(Rm^{-1/3})$, determined by $m\omega'(r) + kW'(r) = 0$. Dynamo action is then developed in the neighbourhood of this *resonant* surface, through an $\alpha\omega$-generating mechanism (for a review, see e.g. Soward 1994; Childress & Gilbert 1995).

3. Formulation of the eigenvalue problem

3.1. *Fourier-analysed equations*

We consider solutions of the induction equation (1.1*a*) of the form

$$\boldsymbol{B}(x, y, z, t) = \mathrm{Re}\,[\boldsymbol{b}(x, y)\exp(pt + \mathrm{i}kz)], \tag{3.1}$$

where the real part of p, denoted below by p^r, is the growth rate of the magnetic field and k the vertical magnetic wavenumber. The horizontal (x, y)-components of the induction equation (1.1*a*) yield the following equation:

$$[(\boldsymbol{u}_H \cdot \nabla_H) + p + Rm^{-1}k^2 + \mathrm{i}kK\psi]\boldsymbol{b}_H = (\boldsymbol{b}_H \cdot \nabla_H)\boldsymbol{u}_H + Rm^{-1}\nabla_H^2 \boldsymbol{b}_H, \tag{3.2}$$

where the subscript H (Z) denotes the horizontal (vertical) components or derivatives. According to (1.1*b*), the vertical component of the magnetic field is given by

$$\nabla_H \cdot \boldsymbol{b}_H = -\mathrm{i}kb_Z. \tag{3.3}$$

Now, decomposing $\boldsymbol{b}_H$ in a Fourier series with respect to both x and y gives

$$\boldsymbol{b}_H = \sum_{m=-\infty}^{+\infty} \sum_{n=-\infty}^{+\infty} (f_{m,n}, g_{m,n}) \exp[\mathrm{i}(mx + ny)], \tag{3.4}$$

where $f_{m,n}$ and $g_{m,n}$ are complex coefficients, and substituting (3.4) into (3.2), the following relations are derived:

$$\begin{aligned} a^{-1}pf_{m,n} = {} & \left(-a^{-1}Rm^{-1}(k^2 + m^2 + n^2) - \mathrm{i}kK\right) f_{m,n} \\ & + \tfrac{1}{4}\left(-\mathrm{i}kK + (m - n - 1)\right) f_{m-1,n-1} + \tfrac{1}{2}(-\mathrm{i}kK - n) f_{m-1,n} \\ & + \tfrac{1}{4}\left(-\mathrm{i}kK + (-m - n + 1)\right) f_{m-1,n+1} + \tfrac{1}{2}(-\mathrm{i}kK + m) f_{m,n-1} \\ & + \tfrac{1}{4}\left(-\mathrm{i}kK + (m + n + 1)\right) f_{m+1,n-1} + \tfrac{1}{2}(-\mathrm{i}kK - m) f_{m,n+1} \\ & + \tfrac{1}{4}\left(-\mathrm{i}kK + (-m + n - 1)\right) f_{m+1,n+1} + \tfrac{1}{2}(-\mathrm{i}kK + n) f_{m+1,n} \\ & - \tfrac{1}{4}\left(g_{m-1,n-1} + g_{m-1,n+1} + 2g_{m,n-1} + 2g_{m,n+1} + g_{m+1,n-1} + g_{m+1,n+1}\right) \end{aligned} \tag{3.5a}$$

and

$$\begin{aligned} a^{-1}pg_{m,n} = &\left(-a^{-1}Rm^{-1}(k^2+m^2+n^2) - \mathrm{i}kK\right) g_{m,n} \\ &+\tfrac{1}{4}\left(-\mathrm{i}kK + (m-n+1)\right) g_{m-1,n-1} + \tfrac{1}{2}(-\mathrm{i}kK - n) g_{m-1,n} \\ &+\tfrac{1}{4}\left(-\mathrm{i}kK + (-m-n-1)\right) g_{m-1,n+1} + \tfrac{1}{2}(-\mathrm{i}kK + m) g_{m,n-1} \\ &+\tfrac{1}{4}\left(-\mathrm{i}kK + (m+n-1)\right) g_{m+1,n-1} + \tfrac{1}{2}(-\mathrm{i}kK - m) g_{m,n+1} \\ &+\tfrac{1}{4}\left(-\mathrm{i}kK + (-m+n+1)\right) g_{m+1,n+1} + \tfrac{1}{2}(-\mathrm{i}kK + n) g_{m+1,n} \\ &+\tfrac{1}{4}\left(f_{m-1,n-1} + 2f_{m-1,n} + f_{m-1,n+1} + f_{m+1,n-1} + 2f_{m+1,n} + f_{m+1,n+1}\right). \end{aligned} \tag{3.5b}$$

A truncation of the system (3.5*b*) is done imposing an integer N such that

$$f_{m,n} = g_{m,n} = 0 \quad \text{if} \quad \max\left(|m|,|n|\right) > N. \tag{3.6}$$

According to Roberts (1972), since all generalized eigenfunctions of (3.5*a*, *b*) satisfy homogeneous linear elliptic differential equations with infinitely differentiable coefficients and periodic boundary conditions, the eigenvalues found numerically are expected to converge as $N \to \infty$. In practice, for each computation, the truncation error is evaluated by

$$\rho = \left(1 - \frac{|\boldsymbol{V}_{N-1}|^2}{|\boldsymbol{V}_N|^2}\right)^{1/2}, \tag{3.7}$$

where $\boldsymbol{V}_N$ is the eigenvector truncated at rank N and $\boldsymbol{V}_{N-1}$ is equal to $\boldsymbol{V}_N$ but for which the components arising from the mode N are replaced by zero. In fact, the whole system (3.5*a*, *b*) becomes numerically expensive when a high level of accuracy is required. In particular, the higher the magnetic Reynolds number is, the more important the small field scales are, and the higher modes must be computed. This is why we prefer to solve smaller sub-systems, derived from the geometrical symmetries of the flow (2.2).

3.2. *Symmetry arguments*

Let us define the operator corresponding to a rotation of $-\pi/2$ in the (x, y)-plane

$$\boldsymbol{T}(\boldsymbol{X}) \longmapsto \boldsymbol{T}^{\boldsymbol{D}}(\boldsymbol{X}) = \boldsymbol{D}^{-1}\boldsymbol{T}(\boldsymbol{D}\boldsymbol{X}) \tag{3.8}$$

with

$$\boldsymbol{D} = \begin{pmatrix} 0 & 1 & 0 \\ -1 & 0 & 0 \\ 0 & 0 & 1 \end{pmatrix} \quad \text{and} \quad \boldsymbol{X} = \begin{pmatrix} x \\ y \\ z \end{pmatrix},$$

then the following relations are always satisfied for any vector field $\boldsymbol{T}_1$ and $\boldsymbol{T}_2$:

$$(\nabla \times \boldsymbol{T}_1)^{\boldsymbol{D}} = \nabla \times (\boldsymbol{T}_1^{\boldsymbol{D}}), \quad (\nabla^2 \boldsymbol{T}_1)^{\boldsymbol{D}} = \nabla^2(\boldsymbol{T}_1^{\boldsymbol{D}}), \quad (\boldsymbol{T}_1 \times \boldsymbol{T}_2)^{\boldsymbol{D}} = \boldsymbol{T}_1^{\boldsymbol{D}} \times \boldsymbol{T}_2^{\boldsymbol{D}}. \tag{3.9}$$

It follows that if $(\boldsymbol{u}, \boldsymbol{B})$ satisfies the induction equation (1.1*a*), then so does $(\boldsymbol{u}^{\boldsymbol{D}}, \boldsymbol{B}^{\boldsymbol{D}})$. Consequently, if $(\boldsymbol{u}_H, \boldsymbol{b}_H)$ satisfies (3.2), then so does $(\boldsymbol{u}_H^{\boldsymbol{D}}, \boldsymbol{b}_H^{\boldsymbol{D}})$. In addition, the flow (2.2) satisfies $\boldsymbol{u}^{\boldsymbol{D}} = \boldsymbol{u}$. It follows that both $\boldsymbol{b}_H$ and $\boldsymbol{b}_H^{\boldsymbol{D}}$ must satisfy the same eigenvalue problem (3.2). Therefore, for a given eigenvalue p, as $\boldsymbol{b}_H$ and $\boldsymbol{b}_H^{\boldsymbol{D}}$ are both eigenvectors they must be constant multiples of each other. This can be written as

$$\boldsymbol{b}_H(x, y) = -C[\hat{\boldsymbol{z}} \times \boldsymbol{b}_H](y, -x), \tag{3.10}$$

where C is a complex coefficient, and in terms of the Fourier coefficients

$$f_{m,n} = C g_{n,-m} \quad \text{and} \quad g_{m,n} = -C f_{n,-m}. \tag{3.11}$$

From (3.11), it follows that $f_{m,n} = C^4 f_{m,n}$, implying that

$$C \in \{1, -1, i, -i\}. \tag{3.12}$$

The four possible values of C, that we shall denote by $C_1, C_{-1}, C_{+\mathrm{i}}$ and $C_{-\mathrm{i}}$, define four families of eigensolutions. Each family can be investigated independently from each other. Inserting (3.11) in (3.5a, b), we can write for each value of C a sub-system of resolution. For given large N, the size of each sub-system is about sixteen times smaller than the size of the full original system (3.5a, b). As a result, an accurate evaluation of the growth rates for values of Rm up to 2^{12} has been possible, requiring a number of modes up to $N = 29$. Some tests have been done in order to check that the union of eigensolutions of the four sub-systems is identical to the set of eigensolutions of the system (3.5a, b). Differences lower than 10^{-4} for the eigenvectors and 10^{-6} for the eigenvalues have been found, the residual error probably coming from the method of derivation of the eigenparameters†. In addition, we can show that the eigensolutions of the four sub-systems also satisfy the following relations:

$$p_{+\mathrm{i}}(k) = p^{\mathrm{c.c.}}_{-\mathrm{i}}(-k), \quad p_{+1}(k) = p^{\mathrm{c.c.}}_{+1}(-k), \quad p_{-1}(k) = p^{\mathrm{c.c.}}_{-1}(-k), \tag{3.13a}$$

$$\boldsymbol{V}_{+\mathrm{i}}(k) = \boldsymbol{V}^{\mathrm{c.c.}}_{-\mathrm{i}}(-k), \quad \boldsymbol{V}_{+1}(k) = \boldsymbol{V}^{\mathrm{c.c.}}_{+1}(-k), \quad \boldsymbol{V}_{-1}(k) = \boldsymbol{V}^{\mathrm{c.c.}}_{-1}(-k), \tag{3.13b}$$

where c.c. denotes complex conjugate. Therefore, it is sufficient to focus on the positive values of k.

Roberts (1972) used similar arguments for his first motion. As he was interested in eigensolutions with a non-zero mean value, he concentrated only on the cases $C = \pm\mathrm{i}$ (C being denoted ω in Roberts (1972)). In this paper, we shall compute the eigensolutions for the four values of C, in order to see whether the mean field solution is dominant or not. The geometrical meaning of the four independent families of eigensolutions will be detailed in §4.2.2.

3.3. *α-effect*

The expression for the kinematic helicity of the flow (2.2)

$$\boldsymbol{u} \cdot \nabla \times \boldsymbol{u} = -w\Delta\psi + \nabla\psi \cdot \nabla w = Ka^2(1 + \cos x)(1 + \cos y)(2 + \cos x + \cos y) \tag{3.14}$$

has a constant sign everywhere (positive as K). It follows that an α-effect is expected which should enable a mean-field dynamo to operate (see e.g. Krause & Rädler 1980). In order to characterize this physical process, the velocity and the magnetic fields are expressed as the sum of a mean part on a periodic cell, denoted by $\langle\ \rangle$, plus a fluctuating part, denoted by $\tilde{}$,

$$\boldsymbol{u} = \langle \boldsymbol{u} \rangle + \tilde{\boldsymbol{u}}, \quad \boldsymbol{b} = \langle \boldsymbol{b} \rangle + \tilde{\boldsymbol{b}}, \tag{3.15}$$

the mean being defined by

$$\langle \cdots \rangle = \int_{-\pi}^{+\pi} \int_{-\pi}^{+\pi} \cdots \mathrm{d}x\, \mathrm{d}y. \tag{3.16}$$

The mean part of the induction equation (1.1a) on a periodic cell is

$$\left(p + Rm^{-1}k^2 + \mathrm{i}kK\langle\psi\rangle\right)\langle \boldsymbol{b} \rangle = \mathrm{i}k\hat{\boldsymbol{z}} \times \langle \tilde{\boldsymbol{u}} \times \tilde{\boldsymbol{b}} \rangle. \tag{3.17}$$

† We used the subroutine CGEEV of the standard LA PACK driver routine (version 1.0).

Clearly, $\hat{\boldsymbol{z}} \times (\tilde{\boldsymbol{u}} \times \tilde{\boldsymbol{b}}) = (\hat{\boldsymbol{z}} \cdot \tilde{\boldsymbol{b}}_Z)\tilde{\boldsymbol{u}}_H - (\hat{\boldsymbol{z}} \cdot \tilde{\boldsymbol{u}}_Z)\tilde{\boldsymbol{b}}_H$. In terms of the Fourier coefficients, we find that

$$\langle(\hat{\boldsymbol{z}} \cdot \tilde{\boldsymbol{u}}_Z)\tilde{\boldsymbol{b}}_H\rangle = \frac{Ka}{4}\big(2(f_{-1,0} + f_{0,-1} + f_{0,1} + f_{1,0}) + f_{-1,-1} + f_{-1,1} + f_{1,-1} + f_{1,1},$$
$$+2(g_{-1,0} + g_{0,-1} + g_{0,1} + g_{1,0}) + g_{-1,-1} + g_{-1,1} + g_{1,-1} + g_{1,1}, 0\big), \quad (3.18)$$

$$\langle(\hat{\boldsymbol{z}} \cdot \tilde{\boldsymbol{b}}_Z)\tilde{\boldsymbol{u}}_H\rangle = \frac{\mathrm{i}a}{4k}\left(\sum_{m,n=-1}^{1} mnf_{m,n} + g_{-1,-1} + g_{-1,1} + 2g_{0,-1} + 2g_{0,1} + g_{1,-1} + g_{1,1},\right.$$
$$\left. - \sum_{m,n=-1}^{1} mng_{m,n} - f_{-1,-1} - f_{-1,1} - 2f_{-1,0} - 2f_{1,0} - f_{1,-1} - f_{1,1}, 0\right). \quad (3.19)$$

From (3.11), we have $(f_{0,0}, g_{0,0}) = -C^2(f_{0,0}, g_{0,0})$, implying that only $C = \pm\mathrm{i}$ can lead to a non-zero mean magnetic field. Furthermore, $g_{0,0} = -Cf_{0,0}$, implying that $\langle\boldsymbol{b}_H\rangle = f_{0,0}(1, -C, 0)$. Then, for $C = \pm\mathrm{i}$, (3.18) and (3.19) simplify in such a way that we can derive two coefficients α_S and α_T satisfying

$$\alpha_S\langle\boldsymbol{b}_H\rangle = \mathrm{i}\langle(\hat{\boldsymbol{z}} \cdot \tilde{\boldsymbol{u}}_Z)\tilde{\boldsymbol{b}}_H\rangle \quad \text{and} \quad \alpha_T\langle\boldsymbol{b}_H\rangle = -\mathrm{i}\langle(\hat{\boldsymbol{z}} \cdot \tilde{\boldsymbol{b}}_Z)\tilde{\boldsymbol{u}}_H\rangle. \quad (3.20)$$

They are given by

$$\alpha_S = \frac{\mathrm{i}Ka}{2f_{0,0}}(2f_{1,0} + 2f_{0,1} + f_{1,1} + f_{1,-1}), \quad (3.21a)$$

$$\alpha_T = \frac{a}{2kf_{0,0}}(-2Cf_{1,0} + (1 - C)f_{1,1} - (1 + C)f_{1,-1}). \quad (3.21b)$$

Therefore, equation (3.17) can be written in the form

$$p + Rm^{-1}k^2 + \mathrm{i}kK\langle\psi\rangle = -k(\alpha_S + \alpha_T). \quad (3.22)$$

The complex coefficients α_S and α_T correspond, respectively, to the relative contribution of the terms $-\mathrm{i}kK\langle\tilde{\psi}\tilde{\boldsymbol{b}}_H\rangle$ and $\langle(\tilde{\boldsymbol{b}}_H \cdot \nabla)\tilde{\boldsymbol{u}}_H\rangle$ in (3.2) to the horizontal mean field generation. Their real parts are related to the stretch and twist mechanisms introduced by Soward (1987).

The term $\mathrm{i}kK\langle\psi\rangle$ in (3.22) expresses the influence of the mean vertical motion on the pulsation of the mean magnetic field (imaginary part of p), upon which a dynamo instability of convective type will form. This is not the case, for example in the Roberts flow for which the pulsation is zero due to the zero mean of the alternated vertical flow.

Now, defining $\alpha = \alpha_S + \alpha_T$ (also called the *generalized* α-effect in Soward 1994), we can show that $\langle\tilde{\boldsymbol{u}} \times \tilde{\boldsymbol{b}}\rangle = -\mathrm{i}C\alpha\langle\boldsymbol{b}_H\rangle$. For a given Rm, we can express α by its Taylor series representation with k adopted as the expansion parameter

$$\alpha(k) = \alpha(0) + k\frac{\partial\alpha}{\partial k}(0) + \ldots. \quad (3.23)$$

The first term is the *usual* α-effect and produces a non-zero mean electromotive force. The term $(\partial\alpha/\partial k)(0)$ has the dimension of a magnetic diffusivity. Now, suppose that the dynamo is of Roberts type (§2.2.1). Then (2.8), obtained in the limit of large Rm, and (3.22) lead to

$$\alpha = O(Rm^{-2/3}) \quad (3.24)$$

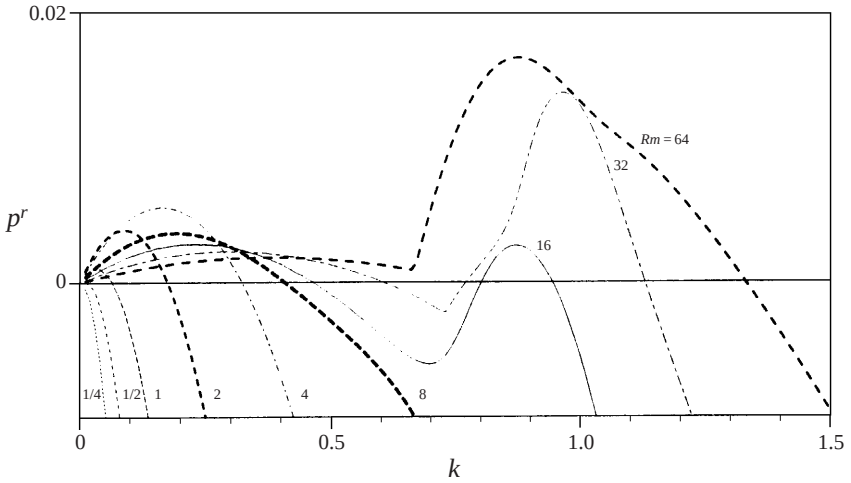

FIGURE 3. Growth rate p^r versus k, for $\chi = 1, C = +i$ and $Rm \in \{2^{-2}, 2^{-1}, 2^0, \ldots, 2^6\}$.

and

$$p = O(Rm^{-1/3}), \quad k = O(Rm^{1/3}). \tag{3.25}$$

In the case of a smooth Ponomarenko-type dynamo (§2.2.2), the relations (3.24) and (3.25) hold, from (2.11) and (3.22).

4. Numerical results

For convenience, we use as control parameters Rm, the magnetic Reynolds number, and χ, the pitch of the solid-body helical motion (u_r, u_θ, u_z) defined in the vicinity of the axis of rotation $x = y = 0$ as introduced in §2.2.2. We express the coefficients K and a in terms of χ, applying the definition $\chi = u_z/(u_\theta)_{r=1}$ and setting $u_r^2 + u_\theta^2 + u_z^2 = 1$. This yields

$$K = \chi/2, \quad a^{-1} = 2(1+\chi^2)^{1/2}. \tag{4.1}$$

With regard to generalization, we note that it is sufficient to concentrate on a given non-zero value of χ, as the eigenparameters for any other value of the pitch, say χ', can be deduced from the following change of variables:

$$k' = \frac{\chi}{\chi'}k, \quad Rm' = \left(\frac{1+\chi'^2}{1+\chi^2}\right)^{1/2} Rm, \quad p' = \left(\frac{1+\chi^2}{1+\chi'^2}\right)^{1/2} \left[p + Rm^{-1}k^2\left(1 - \frac{\chi^2}{\chi'^2}\right)\right]. \tag{4.2}$$

The results below have been obtained for $\chi = 1$.

4.1. *Moderate Rm*

For each value of $C \in \{-\mathrm{i}, +\mathrm{i}, -1, +1\}$, the growth rate p^r has been computed for different values of Rm up to 64. Only the case $C_{+\mathrm{i}}$ (or $C_{-\mathrm{i}}$ with $k < 0$) yields a positive growth rate (figure 3).

For $Rm = 16$, we note that $p^r(k)$ presents two peaks of approximately equal values for $k = 0.23$ and $k = 0.87$, meaning that two dominant modes may coexist. These two solutions correspond to the two dynamo mechanisms introduced in §2.2. This can be seen when plotting the magnetic intensity in the plane (x, y). In figure 4(a), the

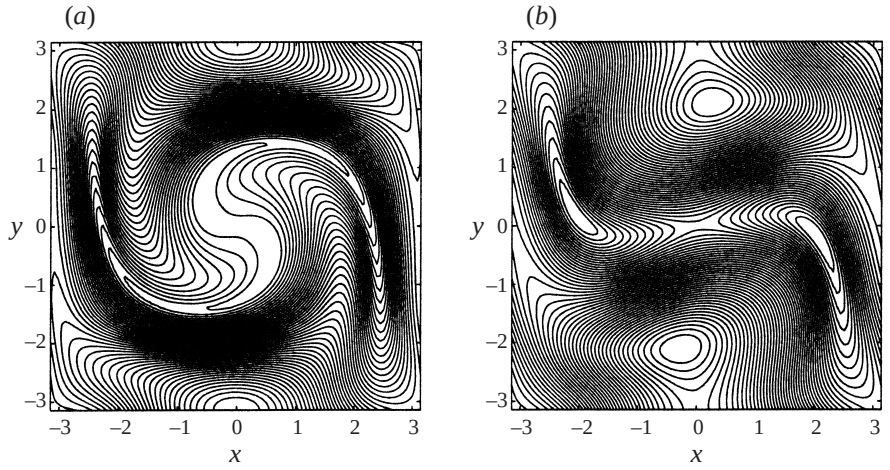

FIGURE 4. Isolines of the magnetic intensity $|b|$ for $Rm = 16$ and (a) $k = 0.23$, (b) $k = 0.87$.

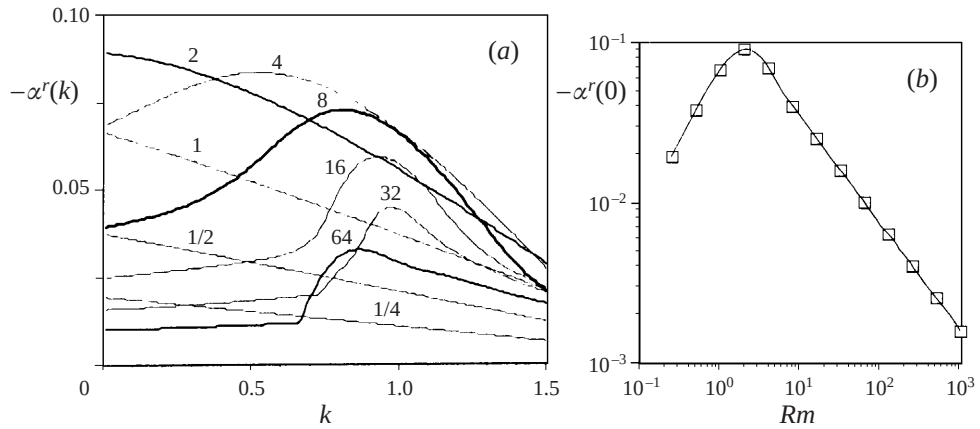

FIGURE 5. (a) *Generalized* α-effect versus k, with the same parameters as in figure 3. (b) *Usual* α-effect ($-\alpha^r(k = 0)$) versus Rm, for $\chi = 1$ and $C = +\mathrm{i}$. It is found that $\alpha^r(k = 0) = O(Rm^{-2/3})$ for large Rm.

magnetic intensity is found to be a maximum at the cell boundaries, corresponding to a Roberts-type dynamo. In figure 4(b), the maximum is located inside the cell, approximately at $x = 0$ and $y = \pm 2$, corresponding to a Ponomarenko-type dynamo with an azimuthal mode $m = 1$. Therefore, there is a competition between the two mechanisms (i.e. the Roberts and Ponomarenko mechanisms) and the dominance of one over the other depends on Rm. The Roberts mechanism is dominant for small Rm and the Ponomarenko mechanism for large Rm, the transition occurring approximately at $Rm = 16$.

The real part of $\alpha(k, Rm)$ is plotted in figure 5(a) for the same values of Rm as in figure 3. On applying (3.23), the *usual* α-effect is deduced for $k = 0$ from these curves (plotted versus Rm in figure 5b). In the limit of large Rm, the *usual* α-effect is found to be $O(Rm^{-2/3})$, as predicted in §3.3.

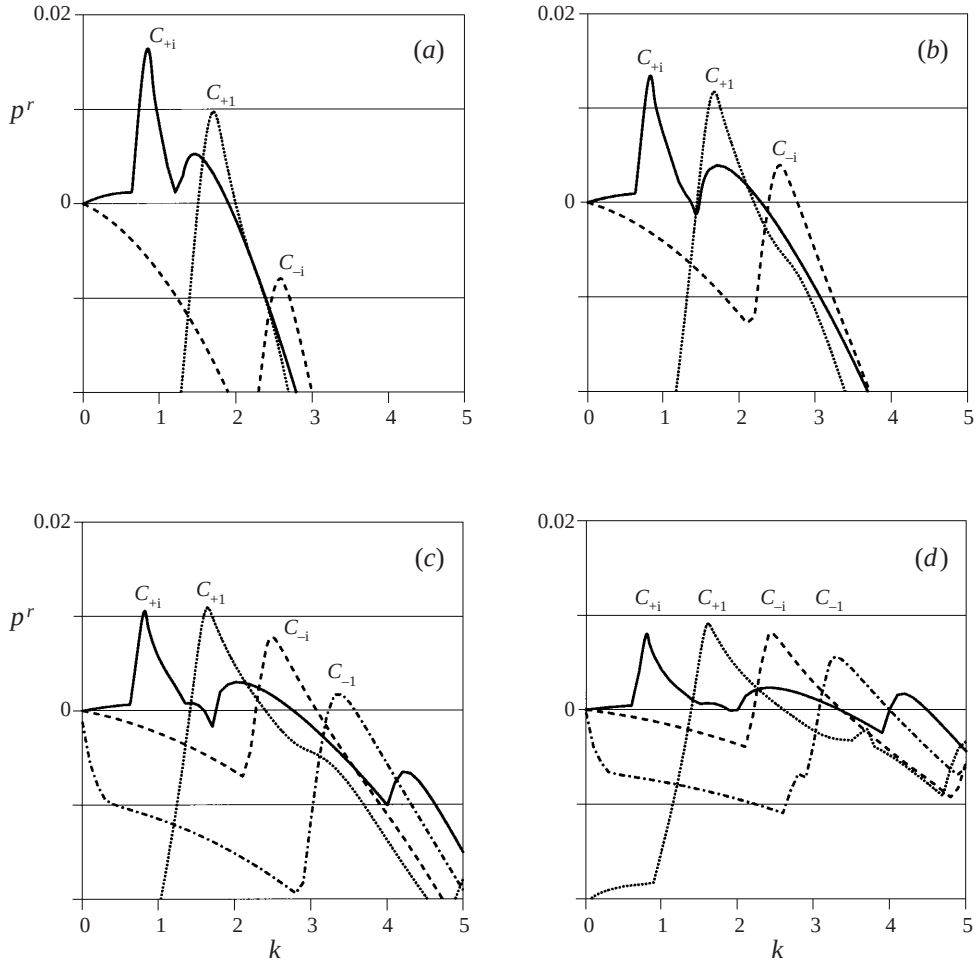

FIGURE 6. Growth rate versus k, for $C \in \{+\mathrm{i}, -\mathrm{i}, +1, -1\}$ and (a) $Rm = 2^8$, (b) $Rm = 2^9$, (c) $Rm = 2^{10}$, (d) $Rm = 2^{11}$.

4.2. *Large Rm*

4.2.1. *Mode crossings*

The results obtained for $Rm \leqslant 64$ show that only C_{+i} yields a non-negative growth rate. Now, for larger values of Rm, the growth rates corresponding to $C_{-\mathrm{i}}, C_{+1}, C_{-1}$ can also be non-negative, depending on k and Rm (figure 6). For each value of C, the maximum growth rate, defined by

$$\gamma(Rm) = \sup_{k \geqslant 0} p^r(k, Rm), \tag{4.3}$$

and the corresponding wavenumber k_γ are plotted, versus Rm, in figure 7(*a*,*b*).

For $Rm = 2^{10}$ and $Rm = 2^{11}$, $\gamma_{C_{+1}}$ is found to be larger than $\gamma_{C_{+\mathrm{i}}}$ (figure 6), implying that the dominant mode does not require an α-effect as C_{+1} corresponds to a zero mean magnetic field. This contrasts with §4.1 in which only a mean-field solution was found. For $Rm = 2^{12}, \gamma_{C_{-\mathrm{i}}}$ becomes dominant (figure 7*a*) and we expect that for larger Rm $\gamma_{C_{-1}}$ will become dominant in turn. Furthermore, the curve $C_{+\mathrm{i}}$ on figure 6 peaks again for $k \approx 4$ suggesting that for higher Rm, $\gamma_{C_{+i}}$ will become dominant again. The

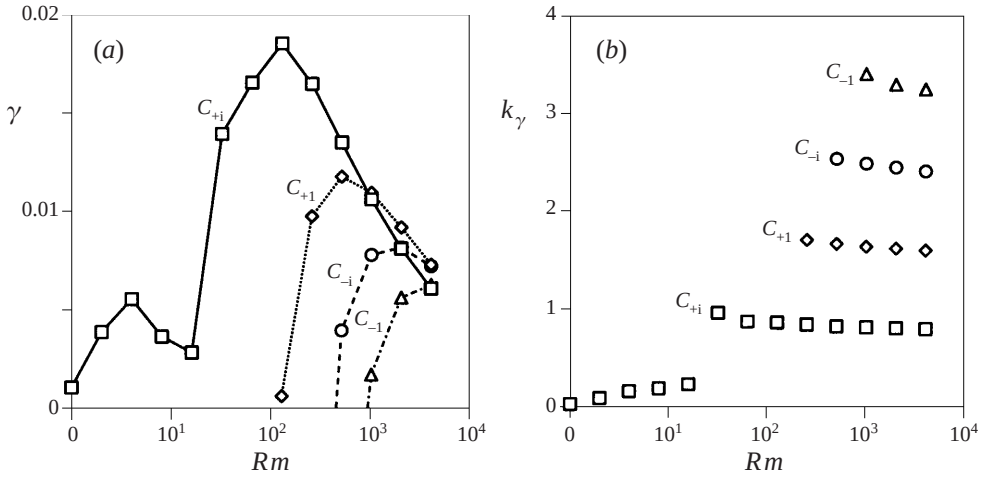

FIGURE 7. The maximum growth rate (*a*) and the corresponding wave number (*b*), versus *Rm*, for $C \in \{+\mathrm{i}, -\mathrm{i}, +1, -1\}$.

wavenumber k_γ takes discrete values at large *Rm* (figure 7*b*), $k_\gamma \in \{0.8; 1.6; 2.4; 3.2\}$. Such mode crossings are in fact typical of a smooth Ponomarenko-type dynamo, as shown below (§4.2.2). Incidentally, figure 7(*a*) suggests that the flow (2.2) is a slow dynamo.

4.2.2. *Helical modes*

In order to describe the geometrical properties of the four subsets of eigensolutions defined by the four values of C, it is convenient to write the $\boldsymbol{b}$-field in the following form:

$$b_x + \mathrm{i}b_y = (b_r + \mathrm{i}b_\theta)\exp(\mathrm{i}\theta), \tag{4.4}$$

where (r, θ, z) are the cylindrical coordinates. Suppose that we have a helical mode as a solution of our problem. Then it can be written

$$\boldsymbol{B} = \mathrm{Re}[\boldsymbol{b}'(r)\exp(pt + \mathrm{i}(kz - m\theta))]. \tag{4.5}$$

This implies that

$$(b_x + \mathrm{i}b_y)(r, \theta) = (b'_r + \mathrm{i}b'_\theta)(r)\exp[\mathrm{i}(1 - m)\theta]. \tag{4.6}$$

In addition, the relation (3.10), derived from the symmetries of the flow (2.2), can be written

$$(b_x + \mathrm{i}b_y)(r, \theta) = -\mathrm{i}C(b_x + \mathrm{i}b_y)(r, \theta - \tfrac{1}{2}\pi). \tag{4.7}$$

Applying (4.6) to each side of (4.7), we find that

$$m + l \equiv 2\,(4), \quad \text{where} \quad C = \mathrm{i}^l,\ l \text{ being integer}. \tag{4.8}$$

As a result, the four independent subsets of eigensolutions correspond to four different families of azimuthal modes, determined as follows:

$$C_{+\mathrm{i}} \quad m \equiv 1\,(4), \tag{4.9a}$$

$$C_{+1} \quad m \equiv 2\,(4), \tag{4.9b}$$

$$C_{-\mathrm{i}} \quad m \equiv 3\,(4), \tag{4.9c}$$

$$C_{-1} \quad m \equiv 4\,(4). \tag{4.9d}$$

This correspondence is confirmed when plotting the magnetic field intensity resulting from the numerical calculations (figure 8*a–e*). Therefore, at large Rm, the smooth Ponomarenko-type dynamo seems to be the dominant mechanism operating. This is also consistent with the constant ratio mentioned in §4.2.1

$$\frac{k_\gamma}{m} \sim 0.8, \tag{4.10}$$

which defines the pitch of the helical magnetic solution and determines the localization of the resonant surface to a neighbourhood within which dynamo action occurs. In figure 8(*a–e*), this surface corresponds to the cylinder $r \approx 1$ on which the $2m$ white islets are distributed.

Figure 8(*f*) shows a Roberts-type dynamo solution for $C_{+\mathrm{i}}$ and $Rm = 2^{11}$. It corresponds to $k = 2.5$ for the curve $C_{+\mathrm{i}}$ of figure 6(*d*). This curve has in fact three maxima: two of Ponomarenko type and one of Roberts type. Though it is not clear in figure 6(*d*), the transition between the different types of solutions is not smooth. There is a discontinuous jump in the slopes as can be also seen in the other curves of figure 6(*a–d*). This differs from the case $Rm = 16$ (figure 3) for which two eigensolutions are plotted in figure 4. Here we can imagine easily a smooth transition leading from one picture to the other upon changing k continuously from 0.23 to 0.87. In figure 9, a diagram is sketched in the parameter space (Rm, k), showing the different types of dynamo, Roberts or Ponomarenko, which can be obtained.

5. Application to the core of an FBR

The velocity field (2.2) has been chosen since it corresponds to features of the flow through the core of an FBR such as helicity and two-dimensional periodicity. However, it may be too simple for the following reasons. For convenience we have modelled the hexagonal array of rods and assemblies in the core by an orthogonal array. The flow in one assembly has at least two scales of helical motion, namely the scales of one rod and one assembly, instead of only one for the flow that we used in (2.2). The global sodium flow inside the reactor is composed of upwards flow in the core but also of downwards flow through the pumps and heat exchangers which is not considered. From this, it follows that, at the scale of the reactor, the dynamo instability may be absolute rather than convective, as mentioned in §3.3. Furthermore, the materials in the core are far from having the same electromagnetic properties as assumed in our model. Some thermoelectric currents have been experimentally measured but are neglected in our calculations. Some assembly housings are ferromagnetic with a permeability 10^3 larger than the assemblies that we considered. Finally, the constituents have different conductivities. The nuclear fuel is made up of PuO_2 and UO_2 which are much poorer conductors than the sodium which flows between the rods. However, it is unclear whether an average conductivity (e.g. based on the relative volume occupied by each constituent) would be meaningful. Anyway, as the core is found to be subcritical in terms of dynamo effect for $\sigma = \sigma_{Na}$, it must be even more so for a lower value of σ resulting from the averaging.

These arguments may certainly change the results presented below. In this respect, our findings should be taken with caution and only as a qualitative insight into the ability of sodium flow, through the core of an FBR, to lead to dynamo action. In any case, an accurate and quantitative approach would demand an intricate knowledge of the three-dimensional sodium flow in a 217-rod assembly which, at present, is not computationally tractable.

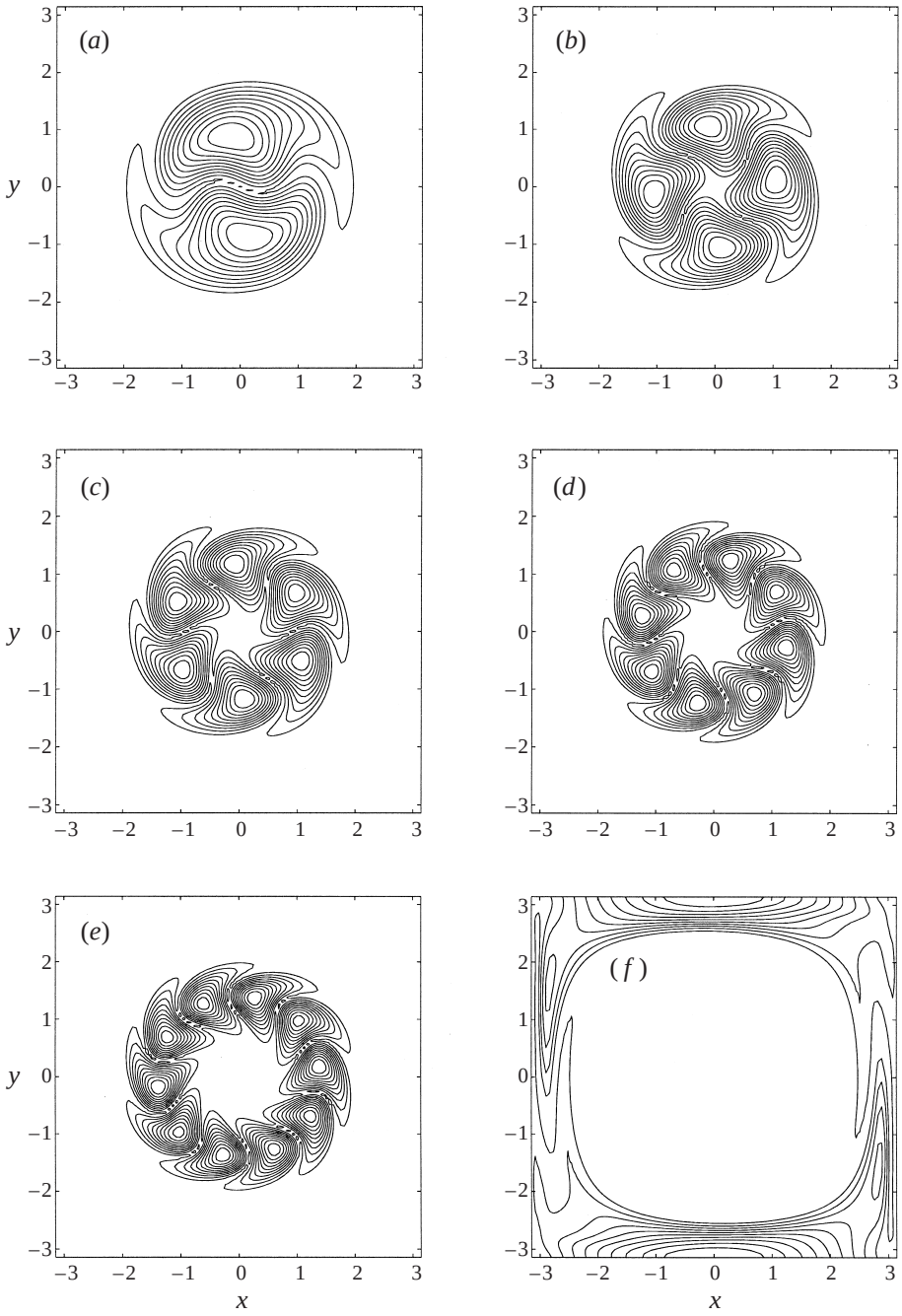

FIGURE 8. Magnetic intensity $|b|$ for $Rm = 2^{11}$ and (*a*) $C_{+\mathrm{i}}, k = 0.8$; (*b*) $C_{+1}, k = 1.6$; (*c*) $C_{-\mathrm{i}}, k = 2.4$; (*d*) $C_{-1}, k = 3.2$; (*e*) $C_{+\mathrm{i}}, k = 4$; (*f*) $C_{+\mathrm{i}}, k = 2.5$.

In table 1, an evaluation of the magnetic Reynolds number (Rm) is presented for a typical length scale of one rod and one assembly corresponding to the FBR Phenix. The characteristic length L and velocity U, appearing in the definition (1.2) of Rm, are expressed in terms of R_0, the mid-distance between the centres of two neighbouring

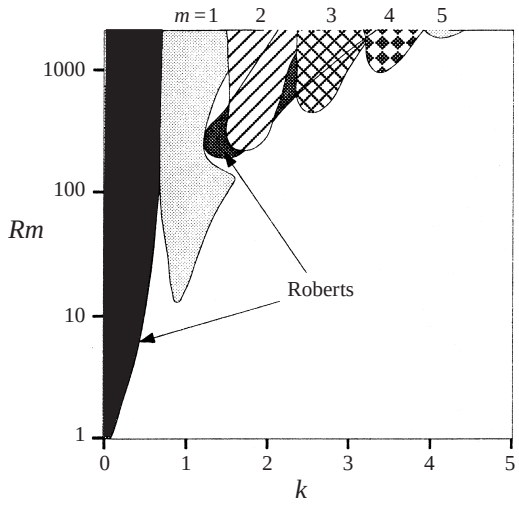

FIGURE 9. Both types of dynamo in the parameter space (k, Rm). The azimuthal mode m is indicated for the dynamo of Ponomarenko type.

	R_0(m)	χ	k_0	Rm	Rm^*
Rod	3.3×10^{-3}	6	3.3×10^{-3}	2.7×10^{-2}	0.4
Assembly	6×10^{-2}	2	6×10^{-2}	0.68	1.1

TABLE 1. Typical parameters at the scale of one rod and one assembly of the FBR Phenix. For $k = k_0$ the marginal Rm is denoted Rm^*. The other data taken for computation are $U_0 = 5$ m s^{-1}, $\sigma = 4 \times 10^6\ \Omega^{-1}$ m^{-1}, $H_0 = 2$ m.

assemblies, and the vertical flow rate U_0 in the core, which has been obtained by direct measurement. The smallest possible value of the magnetic wavenumber k is expressed in terms of the height H_0 of the helical flow in the FBR and is denoted by k_0. The following relations are then derived:

$$L = \frac{1}{\pi} R_0, \quad U = U_0 \frac{(1+\chi^2)^{1/2}}{\chi}, \quad k_0 = 2\frac{R_0}{H_0}, \tag{5.1}$$

where χ is defined as in §2.2.2 and represents the pitch of the sodium motion at the scale of either one rod (χ being equal to the tangent of the space wire angle) or one assembly (χ^{-1} being equal to a relevant ratio U_H/U_Z among those appearing in figure 2).

For $k = k_0$ and for each value of χ given in table 1, the marginal value of Rm (denoted Rm^*) corresponding to a growth rate $p^R = 0$, has been computed and is also included in table 1. The main result is that, at length scales of both one rod and one assembly, the FBR regime is subcritical with respect to dynamo action. However, if the FBR is far from reaching criticality at the scale of one rod, this is less likely at the scale of one assembly. Indeed, the magnetic Reynolds number of the sodium flow is equal to 60% of the critical Rm when considering the scale of one assembly and to 7% when considering the scale of one rod.

6. Discussion

We have analysed the dynamo action in a two-dimensional periodic incompressible flow, made up from identical smooth helical motions. This flow differs from the well-known Roberts flow which is also two-dimensionally periodic but for which the direction of motion alternates between one cell and its immediate neighbour. In both cases, the cell corners are high-order stagnation points but, in contrast with the Roberts 'almost fast' dynamo which only just misses being a fast dynamo with a growth rate $p^r = O(\ln(\ln Rm)/\ln Rm)$ at large Rm, the present flow is 'really slow' with $p^r = O(Rm^{-1/3})$. The magnetic structures are also different. Indeed, whereas the magnetic energy is concentrated in sheets located at the boundaries connecting the hyperbolic stagnation points for the Roberts flow, it is concentrated along resonant cylindrical surfaces within the periodic cells for the present flow. In fact, we have shown that the present flow behaves like a smooth Ponomarenko dynamo at the scale of each periodic cell, with an azimuthal mode $m = O(Rm^{1/3})$.

An heuristic argument to explain such differences with the Roberts flow may rely on the role played by the boundaries. They are the location of the strongest horizontal motion for the Roberts flow and they can enhance the stretching begun in the corners. This is made harder for the present flow as the boundaries are surfaces of zero velocity. As a result, the magnetic energy finds a more efficient location for self-excitation: inside the cell. Another difference, linked also to the flow strength at the boundaries, is the behaviour of the α-effect in the limit of large Rm($\alpha = O(Rm^{-2/3})$ instead of $\alpha = O(Rm^{-1/2})$ for the Roberts flow). But more striking is the existence of zero-mean-field solutions, corresponding to the even azimuthal modes of the helical solutions.

These considerations hold only in the limit of large Rm. Indeed, for $Rm = 16$, both Roberts and Ponomarenko types of solutions may coexist for different values of vertical wavenumbers. In this case, and more generally for moderate Rm, the mean component of the magnetic field is always found to be non-zero.

Concerning the FBR Phenix, the standard regime of the flow through the core has been found to be subcritical. However, though the flow considered has been chosen since it meets general features of the actual sodium flow, such as helicity and two-dimensional periodicity, the possibility remains that it is too simple (see §5).

We gratefully acknowledge Professor A. M. Soward for his stimulating comments and drawing our attention to the helical modes solutions of §4.2.2. We also gratefully acknowledge Professor K.-H. Rädler for helpful comments and having suggested the mathematical formalism of §3.2. The work was supported by the Commissariat à l'Energie Atomique and the Electricité de France, and the article was completed by F. P. whilst being a guest at the Astrophysikalisches Institut of Potsdam, Germany.

REFERENCES

Alemany, A., Marty, P., Plunian, F. & Soto, J. 1998 Experimental investigations of dynamo action in the secondary pumps of the FBR Superphenix. *J. Fluid Mech.* (Submitted).

Bassom, A. P. & Gilbert, A. D. 1997 Nonlinear equilibration of a dynamo in a smooth helical flow. *J. Fluid Mech.* **343**, 375–406.

Bevir, M. K. 1973 Possibility of electromagnetic self-excitation in liquid metal flows in fast reactors. *J. British Nuc. Engng Soc.* **12**, 455–458.

Busse, F. H., Müller, U., Stieglitz, R. & Tilgner, A. 1996 A two-scale homogeneous dynamo: an extended analytical model and an experimental demonstration under development. *Magnetohydrodynamics* **32**, 235–248.

Childress, S. 1979 Alpha-effect in flux ropes and sheets. *Phys. Earth Planet. Int.* **20**, 172–180.

Childress, S. & Gilbert, A. D. 1995 *Stretch, Twist, Fold: The Fast Dynamo*. Springer.

Childress, S. & Soward, A. M. 1989 Scalar transport and alpha-effect for a family of cat's-eye flows. *J. Fluid Mech.* **205**, 99–133.

Gailitis, A. K. 1993 Experimental aspects of a laboratory scale liquid sodium dynamo model. In *Solar and Planetary Dynamos* (ed. M. R. E. Proctor, P. C. Matthews & A. M. Rucklidge), pp. 91–98. Cambridge University Press.

Gailitis, A. K., Karasev, B. G., Kirillov, I. R., Lielausis, O. A., Luzhanskij, S. M., Ogorodnikov, A. P. & Preslitskij, G. V. 1987 *Liquid Metal MHD Dynamo Model*. Physics Institute, Latvian SSR Academy of Sciences.

Gilbert, A. D. 1988 Fast dynamo action in the Ponomarenko dynamo. *Geophys. Astrophys. Fluid Dyn.* **44**, 241–258.

Kirko, I. M., Kirko, G. E., Sheinkman, A. G. & Telichko, M. T. 1982 On the existence of thermoelectric currents in the BN-600 reactor of the Beloyarsk atomic power plant. *Dokl. Akad. Nauk. SSSR* **266**, 854.

Krause, F. & Rädler, K.-H. 1980 *Mean-field Magnetohydrodynamics and Dynamo Theory*. Akademie-Verlag & Pergamon.

Lafay, J., Meunant, B. & Barroil, J. 1975 Local pressure measurements and peripheral flow visualization in a water 19-rod bundle compared with FLICA II B calculations: influence of helical wire-wrap spacer system. *Proc. AICHE-ASME Heat Transfer Conference, California, USA*. ASME.

Moffatt, H. K. 1978 *Magnetic Field Generation in Electrically Conducting Fluids*. Cambridge University Press.

Ponomarenko, Y. B. 1973 On the theory of hydromagnetic dynamo. *Zh. Prikl. Mekh. Tekhn Fiz.* (*USSR*) **6**, 47–51.

Rädler, K.-H., Apstein, E. & Schüler, M. 1997 The Karlsruhe dynamo experiment: a mean field approach. *Proc. 3rd Intl Conf. on Transfer Phenomena in Magnetohydrodynamics and Electroconducting Flows. Aussois, France*.

Roberts, G. O. 1970 Spatially periodic dynamos. *Phil. Trans. R. Soc. Lond.* A **266**, 535–558.

Roberts, G. O. 1972 Dynamo action of fluid motions with two-dimensional periodicity. *Phil. Trans. R. Soc. Lond.* A **271**, 411–454.

Ruzmaikin, A. A., Sokoloff, D. D. & Shukurov, A. 1988 Hydromagnetic screw dynamo. *J. Fluid Mech.* **197**, 39–56.

Soward, A. M. 1987 Fast dynamo action in a steady flow *J. Fluid Mech.* **180**, 267–295.

Soward, A. M. 1989 On dynamo action in a steady flow at large magnetic Reynolds number. *Geophys. Astrophys. Fluid Dyn.* **49**, 3–22.

Soward, A. M. 1990 A unified approach to a class of slow dynamos. *Geophys. Astrophys. Fluid Dyn.* **53**, 81–107.

Soward, A. M. 1994 Fast Dynamos. In *Lectures on Solar and Planetary Dynamos* (ed. M. R. E. Proctor, A. D. Gilbert), pp. 181–217. Cambridge University Press.

Tilgner, A., Busse, F. H. 1995 Subharmonic dynamo action of fluid motions with two-dimensional periodicity. *Proc. R. Soc. Lond.* A **448**, 237–244.

Werkoff, F. & Garnier, J. 1988 Observation of magnetic field generation and distortion in the Phenix liquid-metal fast breeder reactor. *Proc. 5th Beer-Sheva Seminar on MHD Flows and Turbulence 1987, Jerusalem, Israel*. In: *Liquid Metal Flows: Magnetohydrodynamics and Applications* (ed. H. Branover, M. Mond & Y. Unger), *Progress in Astronautics and Aeronautics*, **111**, 349–360. AIAA.